Jour. of the KGS, Vol. 21, No. 7. September 2005, pp. 55~62

# Determination of CPT-based Bearing Capacity of Footings Under Surcharge Using State-dependent Finite Element Analysis

## 상태의존성 유한요소해석 및 CPT결과를 적용한 상재하중하의 얕은 기초의 지지력 결정

Lee, Jun-Hwan[1] 이 준 환
Kim, Dae-Ho[2] 김 대 호
Park, Dong-Gyu[3] 박 동 규

## 요 지

기초지반의 거동은 선형탄성이 아니며, 완전소성상태도 아닌 비선형 응력-변형률의 거동을 보이며, 지반 물성은 하중조건 및 상태에 따라 상이한 값을 나타내게 된다. 기존 기초 지지력 산정방법의 대부분은 기초지반 특성치의 대표값을 적용하고 있어, 응력상태에 따른 지반특성의 변화를 고려하지 못하고 있다. 본 연구에서는 상재하중을 받는 얕은 기초를 대상으로 지반의 상태의존적 변화특성을 고려하며 현장시험결과인 콘지지력값들 적용할 수 있는 얕은 기초의 지지력 산정에 대한 연구를 수행하였다. 이를 위해 상태의존적 응력-변형률 거동 모델을 적용한 비선형 유한요소해석과 콘지지력해석을 수행하였으며, 이를 토대로 콘지지력의 함수로 표시되는 얕은 기초의 지지력 산정방법을 제안하였다. 보다 일반화된 결과를 도출하기 위해 다양한 범위의 상대밀도, 기초의 근입심도 및 크기 등을 고려하여 유한요소해석을 수행하였으며, 이를 통해 얻어진 하중-침하량 곡선을 토대로 콘지지력값으로 정규화된 얕은 기초의 지지력값은 도출하였다. 상재하중이 적용된 지반에서 기초의 근입심도에 따른 정규화 극한 지지력의 차이는 비교적 작은 것으로 나타났으나, 상대밀도에 의한 차이는 큰 것으로 나타났으며, 상대밀도가 증가할수록 얕은 기초의 정규화 지지력은 감소하는 것으로 나타났다.

## Abstract

The use of the bearing capacity equation is subjected to several uncertainties. In this study, estimation of the bearing capacity of footings based on the cone resistance $q_c$ is investigated. Non-linear finite element analyses based on a state-dependent stress-strain model were performed to obtain the load-settlement responses of axially loaded circular footings. Various soil and footing conditions, including different relative densities, depths of embedment, and footing diameters were considered in the analyses. Based on the finite element results, load-settlement curves were obtained and used to determine the unit limit bearing capacity in terms of the cone resistance $q_c$ for footings subjected to surcharge. Values of the unit bearing capacity for different embedment depths were in a narrow range, while considerable variation was observed with relative density $D_R$. It was observed that the unit limit bearing capacity normalized with respect to $q_c$ decreases as $D_R$ increases for a given surcharge.

**Keywords** : Bearing capacity, CPT, Footings, Non-linear stress-strain model, Sands, Surcharge

1 Member, Associate Prof., School of Civil & Environmental Engrg., Yonsei Univ., junlee@yonsei.ac.kr
2 Master student, School of Civil & Environmental Engrg., Yonsei Univ.
3 Member, Ph.D. student, School of Civil & Environmental Engrg., Yonsei Univ.

## 1. Introduction

A common approach to evaluate the bearing capacity of a footing is the use of the bearing capacity equation, which requires knowledge of the shear strength parameters of the foundation soil. Since the full description of the bearing capacity equation was first proposed by Terzaghi (1943), most efforts have been focused on developing more realistic expressions for the bearing capacity factors (Brinch Hansen 1970; Vesic 1973; Michalowski 1997). The use of the bearing capacity equation is subjected to several uncertainties. Significant uncertainties include those associated with assumptions made for the derivation of the bearing capacity equation, which superposition applies, and for the determination of bearing capacity factors.

Other important uncertainty is related to values of the soil friction angle $\phi$. It is known that the friction angle $\phi$ is a function of soil state, varying notably with the stress state and the soil density (Bolton 1986; Been et al. 1991; Bolton and Lau 1993). When a surcharge exists, further variation of the friction angle is expected as the magnitude of the confining stress increases. The experimental procedures available for the estimation of $\phi$ add to the uncertainties. As undisturbed soil sampling is rarely possible in sands, estimation of $\phi$ in general relies on in-situ test results, which introduces their own uncertainties.

In this paper, we study the bearing capacity of circular footings in the presence of surcharge. The study aims at the development of CPT-based bearing capacity estimation method for footings under surcharge. The load response of axially-loaded, circular footings placed on sand and subjected to various surcharge values is obtained using non-linear finite element analysis with a state-dependent stress-strain model and interpreted to obtain the normalized limit unit bearing capacity. A cone resistance analysis is then used to obtain the corresponding cone resistance $q_c$, used to normalize the bearing capacity.

## 2. Uncertainties in the Use of Bearing Capacity Equation

Fig. 1 shows a slip-line pattern typically associated with the bearing capacity failure of a foundation in sand. The bearing capacity equation by Terzaghi (1943) gives the unit load required to generate the slip-line pattern as:

$$q_{bL} = qN_q + \frac{1}{2}\gamma BN_\gamma \quad (1)$$

where $q_{bL}$ = limit unit load at "failure" or limit unit bearing capacity; q = surcharge at footing base level; $\gamma$ = unit weight of foundation soil; B = footing size; and $N_q$ and $N_\gamma$ = bearing capacity factors. The state-dependent shear strength of sands is an uncertain variable for the estimation of the footing bearing capacity. The peak friction angle $\phi_p$ consists of two components, the critical state friction angle $\phi_c$ and a component directly related to the dilatancy angle $\Psi$. While $\phi_c$ is an intrinsic soil variable, the dilatancy angle $\Psi$ is a soil state variable which depends on the relative density $D_R$ and the mean effective stress $\sigma'_m$. The existence of a surcharge causes additional changes in the stress field beneath the foundation and thus changes in the values of $\phi_p$ from what they would be in the absence of a surcharge.

The footing size effect represents additional uncertainty. As the footing size increases, the depth of the influence zone shown in Fig. 1 and the overall confining stress also increase, resulting in lower values of $\phi_p$ due to the reduction in dilatancy.

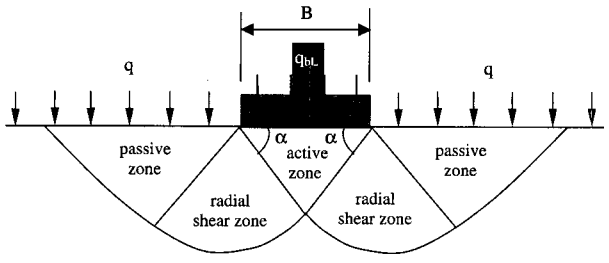


Fig. 1. General slip mechanism of a footing under surcharge. (Das 2002)

## 3. Stress-strain Model

### 3.1 State-dependent Stress-Strain Relationship and Failure Criterion

In the present study, the state-dependent stress-strain model by Lee and Salgado (2000) was adopted for the numerical simulation of the footings on a surcharged sand deposit. The state-dependent stress-strain model used in this study is given by:

$$\frac{G}{G_o}=\left[1-f\left(\frac{\sqrt{J_2}-\sqrt{J_{2o}}}{\sqrt{J_{2\max}}-\sqrt{J_{2o}}}\right)^g\right]\left(\frac{I_1}{I_{1o}}\right)^{n_g} \quad (2)$$

where $G_0$ and G = initial and secant shear modulus; $J_2$, $J_{2o}$, and $J_{2max}$ = current, initial, and maximum second invariants of the deviatoric stress tensor, respectively; $I_1$ and $I_{1o}$ = the first invariants of the stress tensor at the current and initial states, respectively; f and g = material parameters that vary as a function of $D_R$ ; $n_g$ = intrinsic soil variable.

For the description of post-failure behavior, the modified Drucker-Prager failure criterion to allow non-linear elasticity within the failure surface was adopted. The equation for the failure criterion is:

$$\sqrt{J_{2\max}}-\alpha I_1-\kappa=0 \quad (3)$$

where $\alpha$ and $\kappa$ = Drucker-Prager friction and cohesion factors corresponding to $\phi_p$ and c. As discussed previously, the peak friction angle $\phi_p$ is defined in terms of the critical state friction angle $\phi_c$ and the peak dilatancy angle $\Psi_p$. As $\Psi_p$ varies with both relative density and mean effective stress, the failure surface given by (3) is non-linear. In this study, the following relationship proposed by Bolton (1986) was used to estimate the peak friction angle $\phi_p$ in sands:

$$\phi_p=\phi_c+0.8\Psi_p \quad (4)$$

where $\phi_p$ = peak friction angle; $\phi_c$ = critical state friction angle; and $\Psi_p$ = peak dilatancy angle = $6.25I_R$ and $3.75I_R$ for plane-strain and triaxial conditions respectively. The dilatancy index $I_R$ is given by:

$$I_R=I_D\left[Q-\ln\left(\frac{100p'_p}{p_A}\right)\right]-R \quad (5)$$

where $I_D$ = relative density (as a number between 0 and 1); $p_A$ = reference stress = 100 kPa; $p'_P$ = mean effective stress at peak strength in the same units as $p_A$; Q and R= intrinsic soil variables.

### 3.2 Measured and Predicted Footing Load Responses

In order to verify the use of the state-dependent stress-strain model adopted in this study, finite element analyses of footing load tests selected from the literature were performed and compared with measured load-settlement curves. The selected footing load tests are the Texas A&M University load tests reported at / for the

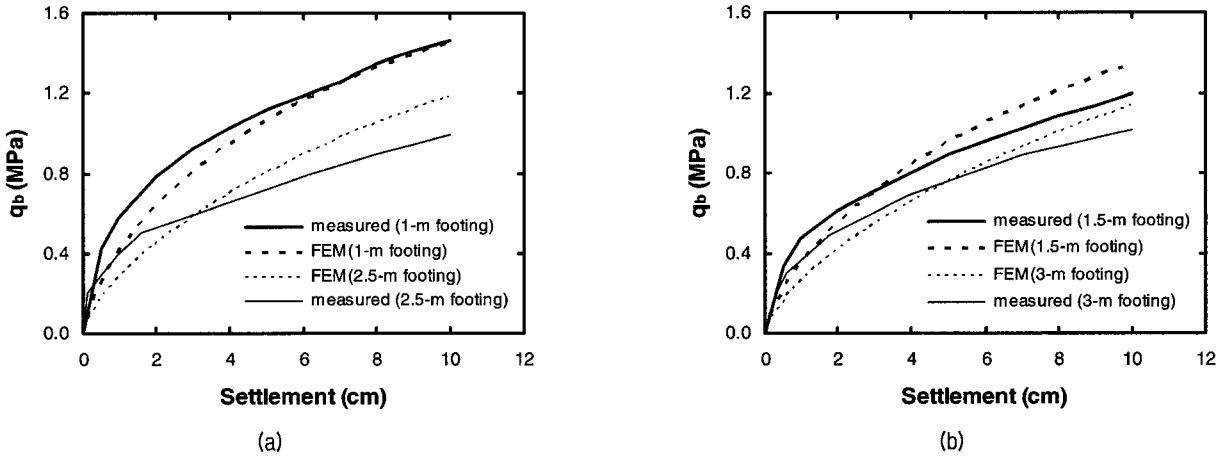


Fig. 2. Measured and predicted load-settlement curves for (a) 1- and 2.5-m footings; and (b) 1.5- and 3-m footings

Settlement '94 ASCE Special Conference (Briaud and Jeanjean 1994).

The commercial finite element program ABAQUS was used with a subroutine written for the state-dependent stress-strain model described previously. Both footings and soils were modeled using twenty-noded 3D solid elements with interface elements between the footing and the surrounding soil. All the soil properties used in the finite element analyses were those obtained from the site characterization and laboratory tests performed before the conference and provided in Briaud and Jeanjean (1994). Fig. 2 shows measured and predicted load-settlement curves for the test footings. As can be seen in the figure, predicted results from the finite element analyses show reasonable agreement with measured results. It is also observed that overestimated loads result from the finite element analysis, compared to measured results, as the settlement level increases.

## 4. Finite Element Simulation of Footings Under Surcharge

Axially-loaded circular footings on sand deposits subjected to a surcharge were modeled using the finite element analysis and the state-dependent stress-strain model. ABAQUS was used for all the analyses. Eight-noded axisymmetric elements were used in the finite element meshes to model both the soil and the footing. The soil was a clean silica sand, whose properties are given in Table 1 (Lee et al. 2004). The parameter $n_g$ used in (2) determines the dependency of confining stress on the modulus degradation. Other necessary parameters used in the analysis are given in Table 2. In Table 2, values of f and g represent characteristics of modulus degradation curves, as explained earlier, and are given as a function of $D_R$ (Lee et al. 2004). Four different relative densities equal to $D_R$ = 30, 50, 70, and 90% and three different footing diameters equal to B = 1, 2, and 3 m were considered in the analyses. The lateral and bottom boundaries of the finite element meshes were located at 12 m horizontally and 15 m vertically from the center of the footing base. Interface elements were used between the footing base and the soil, with a Coulomb friction coefficient equal to 0.7, corresponding to a friction angle equal to around 35°. The surcharge was applied in such a way that the top boundary of surface elements was subjected to a constant pressure corresponding to the magnitude of the surcharge throughout the analysis. The axisymmertic finite element model shown in Fig. 3 was plotted with a visual angle equal to 180° for better visualization.

Fig. 4 shows load-settlement curves for B = 1 m, obtained from the finite element analysis, as a function of relative density $D_R$ and surcharge q under $K_0$ = 0.45. Load-settlement curves for other cases with different footing diameters B were also obtained. As shown in the figure, the load-settlement curves were extended up to a

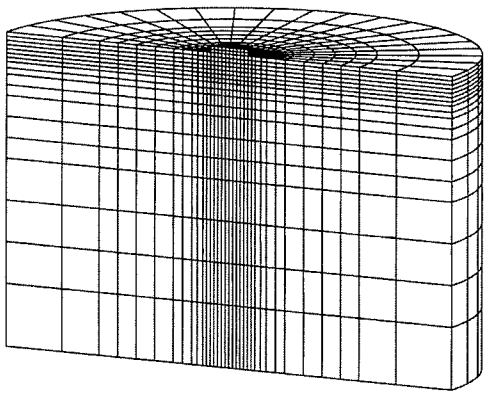

Fig. 3. Finite element model for a circular footing under surcharge

Table 2. Values of f and g used in analysis for different relative density $D_R$

| $D_R$ (%) | 30 | 50 | 70 | 90 |
|---|---|---|---|---|
| f | 0.990 | 0.979 | 0.966 | 0.952 |
| g | 0.118 | 0.259 | 0.386 | 0.496 |

Table 1. Basic properties of sand used in FE analysis

| Sand Type | $e_{min}$ | $e_{max}$ | $\phi_c$ | $G_s$ | $Q^1$ | $R^2$ | $n_g$ | $C_u{}^3$ |
|---|---|---|---|---|---|---|---|---|
| Clean silica sand | 0.48 | 0.78 | 29.5 | 2.65 | 9.9 | 0.86 | 0.44 | 1.48 |

[1,2]Intrinsic soil variables used in Bolton's dilatancy equation
[3]Coefficient of uniformity

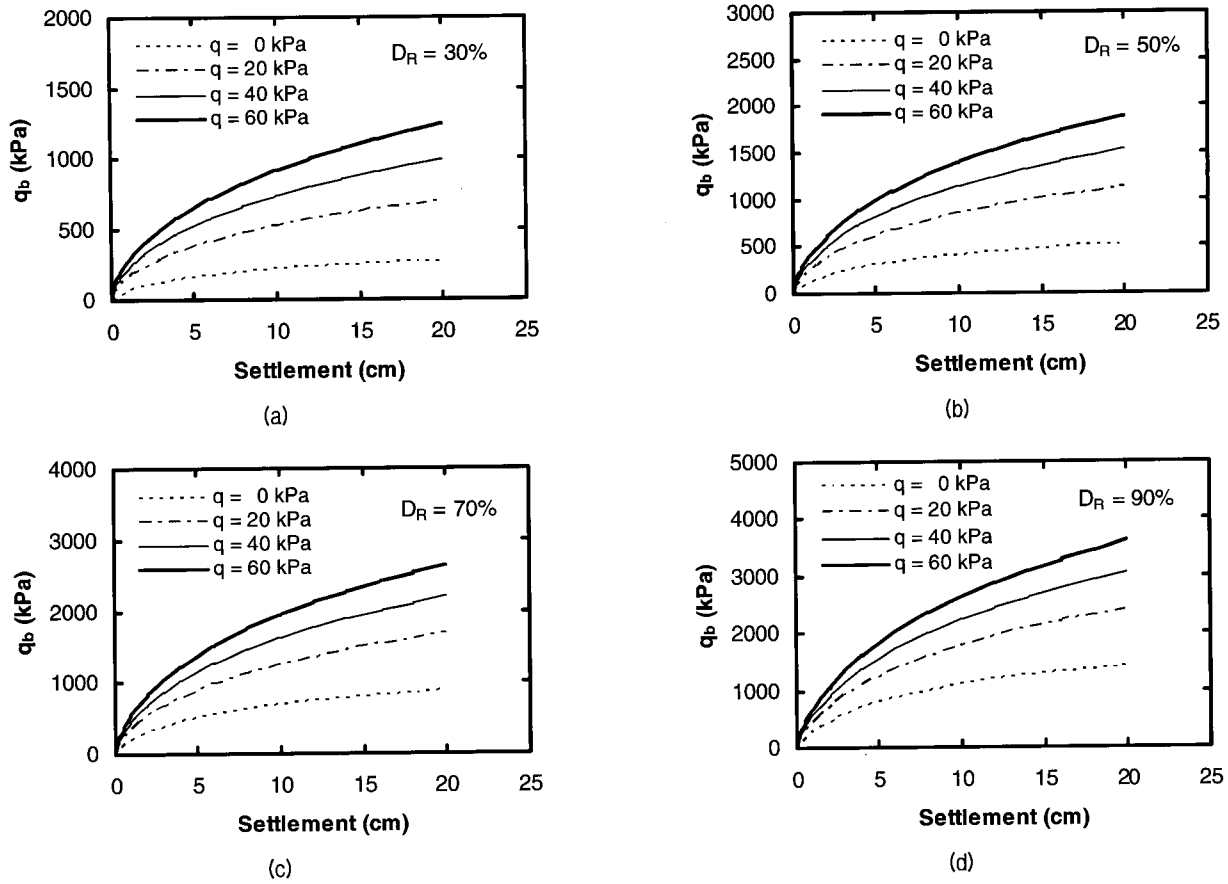


Fig. 4. Load-settlement curves with surcharge for (a) $D_R$ = 30%; (b) $D_R$ = 50%; (c) $D_R$ = 70%; and (d) $D_R$ = 90%

settlement level equal to 20% of the footing diameter B (i.e., s/B = 0.2), corresponding to 20, 40, and 60 cm for the 1-m, 2-m, and 3-m footings, respectively. The footing unit load $q_b$ at s/B = 0.2 is then taken as an approximation to the limit unit bearing capacity $q_{bL}$. From Fig. 4, it is seen that both $D_R$ and q are important factors for the load response and bearing capacity of the footings. As $D_R$ and q increase, the unit load $q_b$ at a given settlement becomes higher.

## 5. Normalized Footing Bearing Capacity with Surcharge

### 5.1 Load-settlement Response of Footings on Soil Subject to a Surcharge

In the present study, the CPT cone resistance $q_c$ was adopted to reduce uncertainties of evaluating the bearing capacity of footings. In order to obtain the footing bearing capacity based on $q_c$, load-settlement curves obtained from the finite element analysis were normalized and replotted in terms of the normalized footing unit load $q_b/q_c$ and the relative settlement s/B. The cone resistance $q_c$ was obtained from penetration resistance and cavity expansion analysis (Salgado et al. 1997). For the normalization, values of the cone resistance $q_c$ from the footing base down to the significant influence zone were averaged. The averaged cone resistance $q_{c,avg}$ was then used to normalize the footing load-settlement curves. The range of the significant influence zone was set to be from footing base to a depth equal the footing diameter B based on the typical critical slip surface for footing.

Fig. 5 shows normalized footing unit load $q_b/q_{c,avg}$ plotted versus relative settlement s/B for a 1-m footing as a function of $D_R$ and q under $K_0$ = 0.45. As shown in the figure, values of $q_b/q_{c,avg}$ at a given s/B increase with increasing $D_R$, as expected, while the effect of surcharge q on the normalized load-settlement curves is small. This is due to similar dependence of $q_c$ and $q_b$ on the confining stress. This result indicates that the nor-

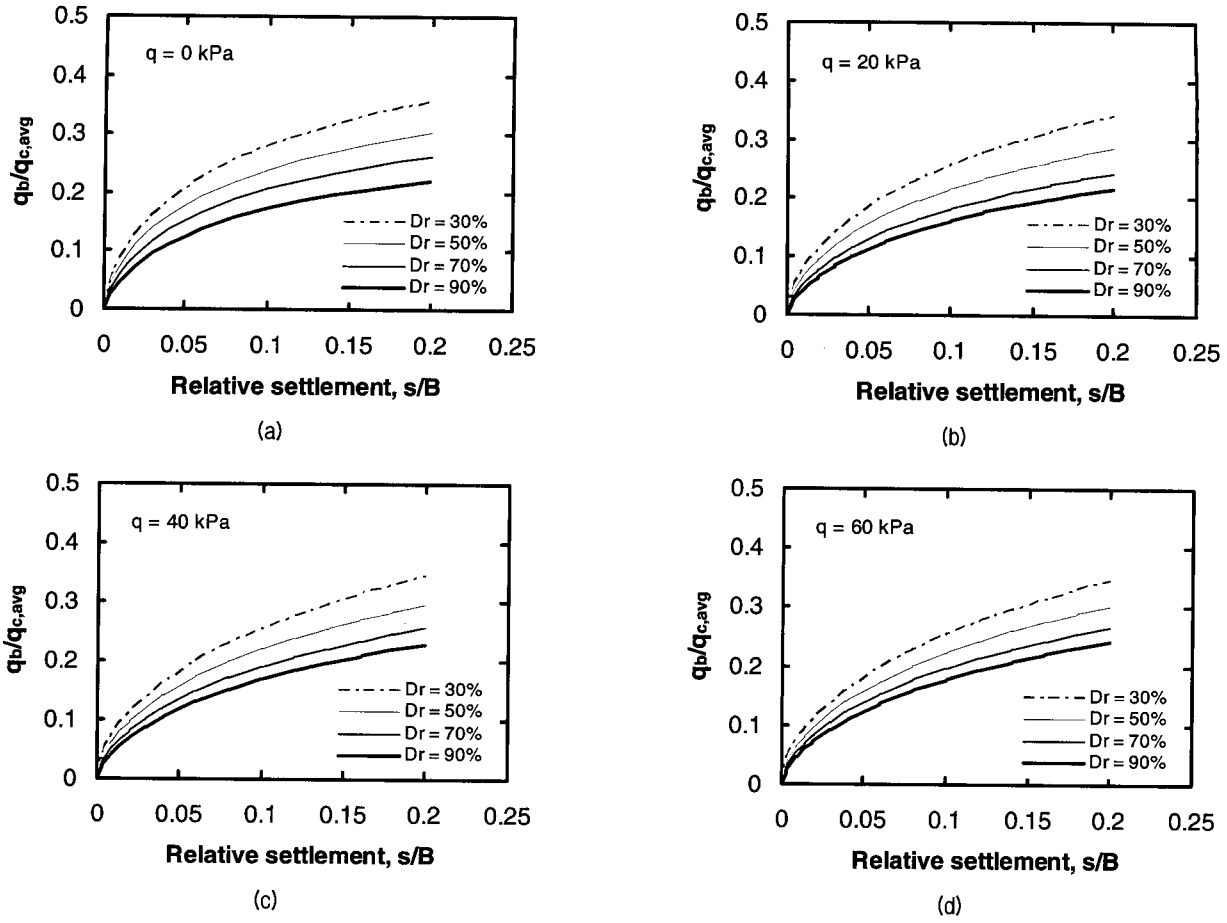


Fig. 5. Normalized load-settlement curves for (a) q = 0 kPa; (b) q = 20 kPa; (c) q = 40 kPa; and (d) q = 60 kPa

malized footing bearing capacity based on $q_c$ may be uniquely determined irrespective of the magnitude of surcharge since the effect of surcharge is already reflected in the value of $q_c$.

## 5.2 Normalized Bearing Capacity of Footings under Surcharge

From the normalized load-settlement curves presented previously, values of normalized limit unit bearing capacity $q_{bL}/q_{c,avg}$ for various soil and footing conditions were obtained. Fig. 6 shows values of $q_{bL}/q_{c,avg}$ as a function of normalized surcharge $q/\gamma B$ for different values of $D_R$. As shown in the figure, while some variations are observed, the range of qbL/qc,avg values for a given DR appears to be quite limited and fairly independent of the surcharge. It is also seen that the $q_{bL}/q_{c,avg}$ decreases as $D_R$ increases. From Fig. 6, for a given value of $q/\gamma B$, larger footings produced higher $q_{bL}/q_{c,avg}$ values. According to the bearing capacity equation by Terzaghi (1943), the limit bearing capacity $q_{bL}$ increases linearly with increasing footing size B, representing the size effect. However, the size effect on $q_{bL}/q_{c,avg}$ is not as significant as on $q_{bL}$ because the process of normalization by dividing $q_{bL}$ by $q_{c,avg}$ partially eliminates the footing size effect. The determination of $q_{c,avg}$, for which the considered influence equal to B increases with increasing footing size B, is itself a way to capture some of this footing size effect.

For the proposed method based on $q_{bL}/q_{c,avg}$ for footings under surcharge, it should be noted that, if the surcharge were applied after placement of the footing, CPT results obtained before and after the application of the surcharge would be different. As a result, the method proposed in this study is limited to cases where CPT results after the placement of the surcharge are available.

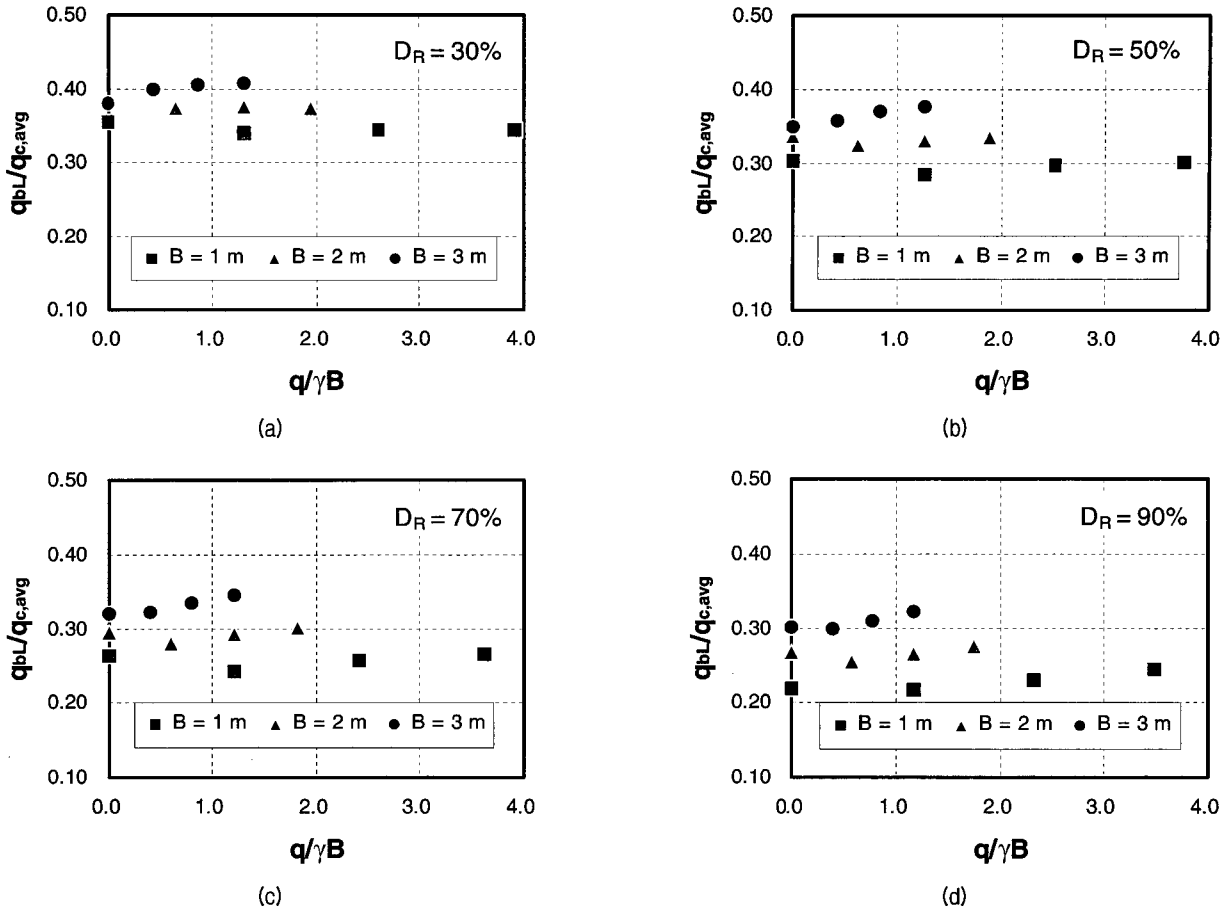


Fig. 6. Values of normalized limit unit bearing capacity $q_{bL}/q_{c,avg}$ with surcharge for (a) $D_R$ = 30%; (b) $D_R$ = 50%; (c) $D_R$ = 70%; and (d) $D_R$ = 90%

## 6. Summary and Conclusions

In this study, 3-D finite element analyses using a state-dependent stress-strain model were performed to investigate the bearing capacity of axially-loaded circular footings resting on sand deposits subjected to a surcharge. Based on the results of the finite element analyses, values of bearing capacity normalized with respect to CPT cone resistance $q_c$ were presented. From the finite element results, load-settlement curves were developed and used to determine the limit unit bearing capacity $q_{bL}$ for various soil and footing conditions. In order to obtain the normalized footing bearing capacity, the load-settlement curves obtained from the finite element analysis were normalized with respect to cone resistance $q_c$. From the normalized load-settlement curves, the normalized limit unit bearing capacity $q_{bL}/q_{c,avg}$ was obtained for various footing and soil conditions.

For a given $D_R$, values of $q_{bL}/q_{c,avg}$ with surcharge q were found to lie in a relatively limited range and to be fairly independent of surcharge values. For a given surcharge, however, larger footings produced greater $q_{bL}/q_{c,avg}$ values. It was also observed that $q_{bL}/q_{c,avg}$ decreases as $D_R$ increases. At $D_R$ = 30 and 90%, the values of $q_{bL}/q_{c,avg}$ fall within 0.34 - 0.41 and 0.22 - 0.32, respectively.

## References


1. Been, K., Jefferies, M.G., and Hachey, J. (1991), "The critical state of sands.", *Geotechnique*, Vol.41, No.3, pp.365-381.
2. Bolton, M. D. (1986), "The strength and dilatancy of sands.", *Geotechnique*, Vol.36, No.1, pp.65-78.
3. Bolton, M. D. and Lau, C. K. (1993), "Vertical bearing capacity factors for circular and strip footings on Mohr-Coulomb soil.", *Canadian Geotechnical Journal*, Vol.30, No.6, pp.1024-1033.
4. Briaud, J. L. and Jeanjean, P. (1994), "Load settlement curve method for spread footings on sand.", *Proceedings of Settlement '94, Vertical*

*and Horizontal Deformations of Foundations and Embankments*, ASCE, Vol.2, pp.1774-1804.

5. Brinch Hansen, J. (1970), *A revised and extended formula for bearing capacity*. Danish Geotechnical Institute, Bulletin No. 28, Copenhagen.
6. Das., B. M. (2002), *Principles of geotechnical engineering*. Brooks/cole, Pacific Groove.
7. Lee, J. H. and Salgado, R. (2000), "Analysis of calibration chamber plate load tests.", *Canadian Geotechnical Journal*, Vol.37, No.1, pp.14-25.
8. Lee, J. H., Salgado, R., and Carraro, A. (2004), "Stiffness degradation and shear strength of silty sands", *Canadian Geotechnical Journal*, Vol.41, No.5, pp.831-843.
9. Michalowski, R. L. (1997), "An Estimate of the influence of soil weight on bearing capacity using limit analysis.", *Soils and Foundations*, Vol.37, No.4, pp.57-64.
10. Salgado, R., Mitchell, J. K., and Jamiolkowski, M. (1997), "Cavity expansion and penetration resistance in sand.", *Journal of Geotechnical and Geoenvironmental Engineering*, ASCE, Vol.123, No.4, pp.344-354.
11. Terzaghi, K. (1943), Theoretical Soil Mechanics, John Wiley & Son, New York, N.Y.
12. Vesic, A. S. (1973), "Analysis of ultimate loads of shallow foundation.", *Journal of the Soil Mechanics and Foundation Division*, ASCE, Vol.99, No.1, pp.45-73.

(received on Jul. 12, 2005, accepted on Sep. 16, 2005)